

conceivable that a quadratic strain dependence of  $T_c$  in combination with an elastic behavior which is close to quadratic could still result in a linear dependence of

$T_c$  upon pressure.

<sup>12</sup>L. R. Testardi and T. B. Bateman, Phys. Rev. **154**, 402 (1967).

## Wavelength Modulation Spectrum of Copper

C. Y. Fong

*Department of Physics, University of California, Davis, California 95616*

and

Marvin L. Cohen,\* R. R. L. Zucca,† J. Stokes, and Y. R. Shen

*Department of Physics, University of California, Berkeley, California 94720, and Inorganic Materials Research Division, Lawrence Radiation Laboratory, University of California, Berkeley, California 94720*

(Received 3 September 1970)

The wavelength modulation spectrum of Cu is presented at 7°K in the range of 2.0  $\leq \hbar\omega \leq 6.0$  eV. The band structure of Cu calculated by the empirical pseudopotential method is used to compute the imaginary part of the dielectric function  $\epsilon_2(\omega)$  and the logarithmic derivative of the reflectivity,  $R'(\omega)/R(\omega)$ . Good agreement between theory and experiment is obtained at the absorption edge and at higher energies using the one-electron approximation if dipole matrix elements are calculated from wave functions including core contributions rather than the pseudowave functions. The transitions causing the structure in  $R'(\omega)/R(\omega)$  are identified.

Recent advances in optical derivative spectroscopy have helped significantly in obtaining detailed knowledge about the band structure of semiconductors.<sup>1</sup> Applications of this technique to metals, however, have been scarce. There have been measurements of the electroreflectance of Ag and Au,<sup>2</sup> but there is some uncertainty<sup>3</sup> associated with the interpretation of these results. Thermoreflectance and piezoreflectance<sup>4</sup> have yielded valuable information about noble-metal band structure, and in the case of piezoreflectance the deformation potentials of Cu were measured. In this Letter, we present the wavelength modulation spectrum of Cu from 2.0 to 6.0 eV taken at 7°K. To our knowledge, this is the first application of wavelength modulation spectroscopy to metals at low temperatures. Our derivative spectrum of Cu shows clearly better resolution than those obtained by other methods. The experimental setup was described briefly elsewhere.<sup>5</sup> The Cu sample used in our measurements was the same single crystal used in cyclotron resonance experiments by Kip, Langenberg, and Morre.<sup>6</sup> After electropolishing the surface, the sample was quickly transferred to the low-temperature Dewar to avoid surface contamination. The sample temperature could be varied easily from 7 to 300°K. Here, for the sake of clarity, we present in Fig. 1 only the

Cu-derivative spectrum taken at 7°K. We have also measured the normal reflectivity spectrum of Cu which agrees well with that of Gerhardt.<sup>4</sup>

The origin of most of the structure in the measured derivative spectrum of Cu can be determined using the theoretical band structure of Cu, calculated by the empirical pseudopotential method.<sup>7</sup> In the calculation we used four form factors for the local pseudopotential and four other pa-

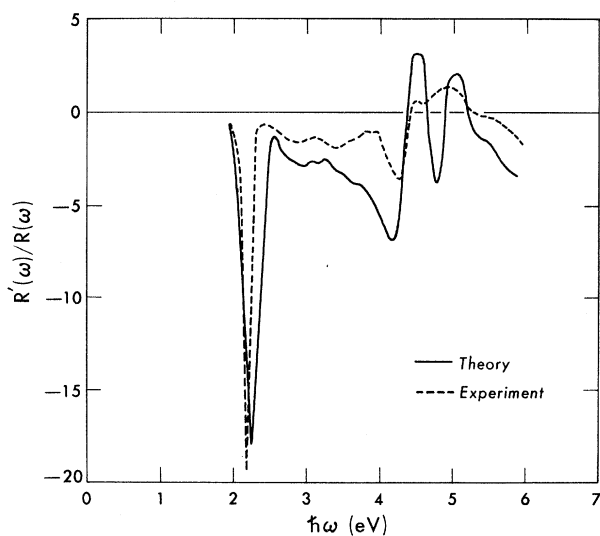


FIG. 1. The measured  $R'(\omega)/R(\omega)$  at  $T=7^\circ\text{K}$  and the calculated  $R'(\omega)/R(\omega)$ .

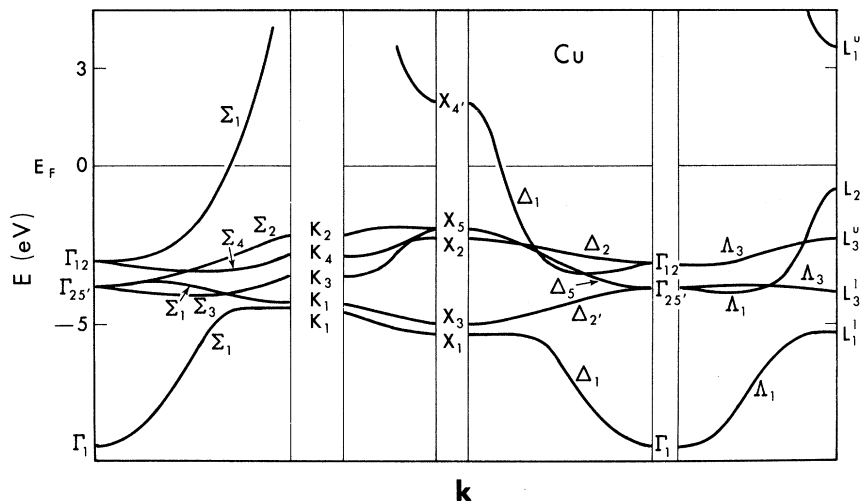


FIG. 2. Band structure of Cu.

rameters relating to a nonlocal pseudopotential with  $l=2$ . These eight parameters are determined by fitting to the optical data obtained by Gerhardt<sup>4</sup> and the photoemission data of Spicer.<sup>8</sup> Because of the complication in defining the parameters for the nonlocal pseudopotential, we give only the local form factors:  $V(|\vec{G}|^2=3) = 0.0131$ ,  $V(4) = 0.0189$ ,  $V(8) = 0.0162$ , and  $V(11) = 0.0014$  Ry. [In Ref. 7,  $V(4)$ ,  $V(8)$ , and  $V(11)$  were inadvertently omitted.] The parameters related to the nonlocal pseudopotential are defined and their values are given in Ref. 7. The lattice constant of Cu is  $3.61 \text{ \AA}$ . The resulting band structure is shown in Fig. 2. We have shifted the Fermi level upward by  $0.25 \text{ eV}$  compared with the results given in Ref. 7. In this way, the

first peak relative to  $E_F$  of the density of states for the  $d$  bands is at  $-2.25 \text{ eV}$ . Most of the structure in the density of states agrees with more recent photoemission data by Krowlikowski and Spicer<sup>9</sup> and by Smith<sup>10</sup> to an accuracy of  $0.1 \text{ eV}$ . The radii of the Fermi surface along  $[100]$ ,  $[110]$ , and  $[111]$  are  $1.41$ ,  $1.32$ , and  $0.29 \text{ \AA}^{-1}$ . The measured values by Shoenberg<sup>11</sup> are  $1.40$ ,  $1.38$ , and  $0.28 \text{ \AA}^{-1}$ .

The imaginary part of the dielectric function  $\epsilon_2(\omega)$  (constant dipole matrix elements are not assumed; they are computed directly from the pseudowave functions) is calculated by the method described in Saslow *et al.*<sup>12</sup> with a mesh of 89 points in  $1/48$ th of the Brillouin zone. The results are shown in Fig. 3, accompanied by the

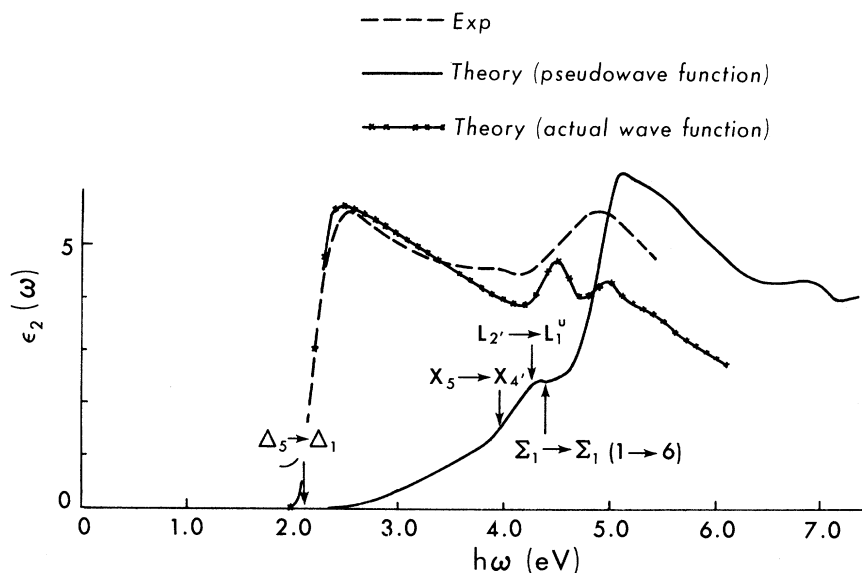


FIG. 3. The measured  $\epsilon_2(\omega)$  and the calculated  $\epsilon_2(\omega)$ .

experimental curve measured by Gerhardt.<sup>4</sup> The agreement between theory and experiment near the 5-eV region is good. However, this  $\epsilon_2(\omega)$  is about an order of magnitude less than the experimental results near 2.0 eV. This suggests either that the dipole matrix elements used in the calculation are not accurate or some kind of enhancement is present in that region.

An enhancement (e.g., indirect processes) involving the product of valence and conduction-band density of states is excluded. As shown in Ref. 7 there is virtually no structure in the conduction-band density of states. The valence band has structure at -2.25, -3.8, and -4.5 eV, measured with respect to the Fermi surface. The largest peak is at 3.8 eV. The product of valence and conduction-band density of states would rise sharply at  $\hbar\omega = 2.25, 3.8$  eV. However, the slope of the product with respect to the photon energy would be positive because of the structureless character of the conduction-band density of states. The corresponding  $R'(\omega)/R(\omega)$  would therefore have a positive value instead of negative value as obtained by the experiment between  $2.0 \leq \hbar\omega \leq 4.0$  eV.

Our matrix elements can, however, be inaccurate because the pseudowave functions with *s* and *p* character are not orthogonal to the inner-core states. The importance of using wave functions including core contributions instead of pseudowave functions to calculate the dipole matrix elements in metals has been recognized by Muller and Phillips<sup>13</sup> and by Animalu and Harrison.<sup>14</sup> Our treatment is different from theirs in that the core contributions are explicitly included. The actual wave function of the conduction electron is

$$\psi(\vec{r}) = N^{-1} \{ \varphi(\vec{r}) - \sum_b \varphi_b \langle \varphi_b | \varphi \rangle \}, \quad (1)$$

where  $\varphi(\vec{r})$  is the pseudowave function. The  $\varphi_b$ 's are the wave functions for the core states and *N* is the normalization constant. In this work, we take  $\varphi_b$  to be tight-binding wave functions of 3*s* and 3*p* states. The 3*s* and 3*p* states are approximated by hydrogenic wave functions with effective atomic number,  $Z_{eff}$ , equal to 13.5. The  $\epsilon_2(\omega)$  with matrix elements calculated using  $\psi(\vec{r})$  is shown in Fig. 3. It is in excellent agreement with the experimental result. The value of  $Z_{eff} = 13.5$  roughly corresponds to the minimum value of *Z* such that the overlap between neighboring cells for the tight-binding wave functions can be neglected. The agreement between theory and experiment for  $\epsilon_2(\omega)$  at the absorption edge is so

encouraging that one may be motivated to use this approach to resolve the discrepancies between theory and experiment in the optical spectra of alkali metals.

To calculate  $R'(\omega)/R(\omega)$ , we use the interband  $\epsilon_2(\omega)$  in Fig. 3 calculated using the  $\psi(\vec{r})$  wave functions and add to this the free-electron Drude contribution as discussed by Ehrenreich and Cohen.<sup>15</sup> The free-electron contribution to the dielectric function  $\epsilon^f(\omega)$  calculated from Drude theory is<sup>16</sup>

$$\epsilon^f(\omega) = 1 - 4\pi n e^2 [m^* \omega(\omega + i/\tau)]^{-1}, \quad (2)$$

where *n*, *e*, and *m\** are the density, charge, and effective mass of the free electrons, respectively. We use  $m^* = 1.42m_0$  which is estimated at the belly using the matrix elements of the present calculation; the measured value by Schulz<sup>17</sup> is  $1.45m_0$ , where  $m_0$  is the bare electron mass.  $\tau$  is the relaxation time and its value is approximately  $2.0 \times 10^{-14}$  sec.<sup>16,18</sup> With the quoted value of  $\tau$ , we can neglect the imaginary part of  $\epsilon_2^f(\omega)$ .

The  $R'(\omega)/R(\omega)$  is then calculated by the method described in Walter and Cohen<sup>19</sup> and is plotted in Fig. 1. The general structure of the calculated and the experimental  $R'(\omega)/R(\omega)$  agrees very well. There is some discrepancy in the magnitude of the two results. The interband transitions start at 2.1 eV. Most of the transitions near this energy come from  $\Delta_5 - \Delta_1(5-6, 4-6)$  and all transitions from the fifth band to the Fermi surface. We shall refer to these points in  $\vec{k}$  space as osculating points (using the nomenclature of Mueller and Phillips<sup>13</sup>). The structure near 3.2 eV arises mainly from a large volume effect of 5-6 and 4-6 transitions. The corresponding contours of the energy difference between the sixth band and the fourth and fifth bands are roughly parallel to the Fermi surface. The contour will intersect along  $\Delta$  very close to *X*. The calculated  $R'(\omega)/R(\omega)$  shows some small structure at 3.7 eV; the measured curve has a twin-peaks structure at 3.8 and 3.95 eV. The contribution to this structure comes from an osculating point  $\Sigma_1 - \Sigma_1(3-6)$  and a large volume effect from 5-6, 4-6, and 3-6 transitions with energy contours close to the Fermi surface. The effect of a critical point with  $M_1$  symmetry at 3.96 eV from  $X_5 - X_4'$  transition does not show up clearly in the calculated  $R'(\omega)/R(\omega)$  but does show up in the calculated  $\epsilon_2(\omega)$ . We associate it with the upper structure of the twin peaks in the experimental results. The first zero in the calculated  $R'(\omega)/R(\omega)$  is at 4.37 eV which is in ex-

Table I. Identification of the important interband transitions of Cu.

Transitions	Energy (eV)	Symmetry
$\Delta_5 \rightarrow \Delta_1$ (5 $\rightarrow$ 6, 4 $\rightarrow$ 6) and all the transitions from 5-th band to the Fermi surface.	2.1	Osculating point <sup>a</sup> Osculating points
Large (5 $\rightarrow$ 6)(4 $\rightarrow$ 6) transition region inside the BZ near X and the Fermi surface	3.2	Volume effect
$\Sigma_1 \rightarrow \Sigma_1$ (3 $\rightarrow$ 6)	3.7	Osculating point
Large(5 $\rightarrow$ 6)(4 $\rightarrow$ 6) and (3 $\rightarrow$ 6) transition region inside BZ near X and the Fermi surface.	3.7	Volume effect
$X_5 \rightarrow X_4'$ (4 $\rightarrow$ 6)(5 $\rightarrow$ 6)	3.96	$M_1$
$L_2' \rightarrow L_1''$ (6 $\rightarrow$ 7)	4.25	$M_0$
$\Sigma_1 \rightarrow \Sigma_1$ (1 $\rightarrow$ 6)	4.38	Osculating point
Large (5 $\rightarrow$ 6), (4 $\rightarrow$ 6) and (3 $\rightarrow$ 6) transitions inside BZ near the Fermi surface.	4.5	Volume effect
Large (2 $\rightarrow$ 6) (1 $\rightarrow$ 6) transitions inside BZ near the Fermi surface.	5.0	Volume effect

<sup>a</sup>Follow the definition in Ref. 13.

cellent agreement with the experimental value of 4.4 eV. Both  $R'(\omega)/R(\omega)$  curves in Fig. 1 show two structures for photon energy  $4.0 \leq \hbar\omega \leq 5.5$  eV. The lower-energy structure starts with  $L_2' \rightarrow L_1''$  transitions at 4.25 eV, resulting from an  $M_0$  singularity and  $\Sigma_1 \rightarrow \Sigma_1$  (1 $\rightarrow$ 6) transition at 4.38 eV which is an osculating point. These critical points contribute structure over a background caused by a large volume effect which is mainly from (5 $\rightarrow$ 6), (4 $\rightarrow$ 6), and (3 $\rightarrow$ 6) transitions in the region near the Fermi surface inside the Brillouin Zone (BZ). The contribution to the upper energy structure comes mainly from the volume effects of 1 $\rightarrow$ 6 and 2 $\rightarrow$ 6 transitions near the Fermi surface. This composite structure ends at 5.3 eV experimentally. The calculated  $R'(\omega)/R(\omega)$  has a corresponding zero at 5.2 eV. The two zeros agree very well. Our results strongly support the comment made recently by Phillips<sup>20</sup> that the 5.0-eV peak in the measured  $\epsilon_2(\omega)$  consists of a threshold at 4.3 eV coming from  $L_2' \rightarrow L_1''$  and a shoulder at 4.8 eV corresponding to

$d$ -band to Fermi-surface transitions. However, our identification for the upper structure shows that it is mainly a volume effect and is not from osculating points. The identifications are summarized in Table I.

In conclusion the agreement between the theoretical and experimental  $R'(\omega)/R(\omega)$  and  $\epsilon_2(\omega)$  enables us to confirm: (a) the optical transitions in Cu are direct as concluded by Smith<sup>10</sup>; (b) the identification of  $X_5 \rightarrow X_4'$  agrees with the result given by Mueller and Phillips<sup>13</sup> and the comments on the composite nature of the 5.0-eV peak in  $\epsilon_2(\omega)$  by Phillips.<sup>20</sup> However, the upper energy structure arises from volume effects. (c) Strong many-body effects are not necessary to obtain agreement between experiment and theory near the absorption edge. (d) The volume-effect contributions to the optical properties of Cu are more important than the critical points at the symmetry points and along the symmetry lines. In addition, our present approach to the dipole matrix elements may be used to resolve the discrepancy between theory and experiment at the absorption edge for alkali metals.

We would like to thank Professor A. F. Kip for making the copper crystal available to us. Thanks are due to Dr. J. C. Phillips for a very helpful discussion during a crucial stage of the calculation. We would like to thank Professor L. M. Falicov for helpful discussions. We also thank J. P. Walter for the use of his program in calculating  $R'(\omega)/R(\omega)$ . Part of this work was done under the auspices of the U. S. Atomic Energy Commission.

\*Work supported in part by the National Science Foundation.

†Fellow, Consejo Nacional de Investigaciones Cientificas y Technicas, Argentina.

<sup>1</sup>See, for example, M. Cardona, *Solid State Phys.*, Suppl. No. 11 (1969).

<sup>2</sup>J. Feinlieb, *Phys. Rev. Lett.* **16**, 1200 (1966); W. N. Hansen and A. Prostak, *Phys. Rev.* **174**, 500 (1968).

<sup>3</sup>B. J. Parson, *Phys. Rev.* **182**, 975 (1969).

<sup>4</sup>W. J. Scower, *Phys. Rev. Lett.* **18**, 445 (1967).  
U. Gerhardt, D. Beaglehole, and R. Sandrock, *Phys. Rev. Lett.* **19**, 309 (1967); U. Gerhardt, *Phys. Rev.* **172**, 651 (1968).

<sup>5</sup>R. R. L. Zucca and Y. R. Shen, *Phys. Rev. B* **1**, 2668 (1970).

<sup>6</sup>A. F. Kip, D. N. Langenberg, and T. W. Moore, *Phys. Rev.* **124**, 359 (1961).

<sup>7</sup>C. Y. Fong and M. L. Cohen, *Phys. Rev. Lett.* **24**, 306 (1970).

<sup>8</sup>W. E. Spicer, in *Proceedings of the International*

*Colloquium on Optical Properties and Electronic Structure of Metals and Alloys, Paris, 13-16 September 1965*, edited by F. Abeles (North-Holland, Amsterdam, 1966).

<sup>8</sup>W. F. Krowlikowski and W. E. Spicer, Phys. Rev. **185**, 882 (1969).

<sup>10</sup>N. V. Smith, to be published.

<sup>11</sup>D. Shoenberg, Phil. Mag. **5**, 105 (1960).

<sup>12</sup>W. Saslow, T. K. Bergstresser, C. Y. Fong, M. L. Cohen, and D. Brust, Solid State Commun. **5**, 667 (1967).

<sup>13</sup>F. M. Mueller and J. C. Phillips, Phys. Rev. **157**, 600 (1967).

<sup>14</sup>A. O. E. Animalu and W. A. Harrison, Bull. Amer. Phys. Soc. **12**, 415 (1967).

<sup>15</sup>H. Ehrenreich and M. H. Cohen, Phys. Rev. **115**, 786 (1959).

<sup>16</sup>H. Ehrenreich and H. R. Phillip, Phys. Rev. **128**, 1622 (1962).

<sup>17</sup>L. G. Schulz, Phil. Mag., Suppl. **6**, 102 (1957).

<sup>18</sup>See, for example, C. Kittel, *Introduction to Solid State Physics* (Wiley, New York, 1966), 3rd ed., p. 228.

<sup>19</sup>J. P. Walter and M. L. Cohen, Phys. Rev. **183**, 763 (1969).

<sup>20</sup>J. C. Phillips, Phys. Rev. **187**, 1175 (1969).

## Even-Parity Levels of Donors in Si<sup>†</sup>

W. H. Kleiner\* and W. E. Krag

Lincoln Laboratory, Massachusetts Institute of Technology, Lexington, Massachusetts 02173

(Received 24 August 1970)

Fifteen excited "even-parity" levels of donor impurities in Si are identified. Observed photoexcitation to these levels in violation of electric-dipole selection rules is attributed to effects of polarization of the donor by other defects and to breakdown of the effective-mass approximation.

In this Letter we identify fifteen peaks in the absorption spectra of seven donor centers in Si with (transitions to) levels having even parity in the effective-mass approximation (EMA).<sup>1</sup> The binding energies of these levels,<sup>2-11</sup> as well as two excited and seven ground even-parity levels previously identified,<sup>3-10</sup> are given in Table I,<sup>12-15</sup>

together with corresponding binding energies<sup>16</sup> calculated<sup>12</sup> in the EMA. Figure 1 shows these levels graphically in relation to nearby *p* levels.<sup>2-12</sup> We have typically identified an observed level with the nearest effective-mass (EM) level, a procedure which can be carried out with little ambiguity and which can be justified by the fol-

Table I. Observed and EM binding energies (in MeV) of some even-parity donor levels in Si. Newly identified levels are indicated by an asterisk. When more than one reference is cited for an entry, the tabulated value is determined from the first reference, which usually gives the sharpest absorption peak, although values from other references usually agree within experimental error.

	Ground	2s	3s	3d <sub>0</sub>
EM <sup>a</sup>	31.27	8.83	4.75	3.75
P	45.54 <sup>b-d</sup>			4.1 ± 0.03* <sup>d,c</sup>
As	53.76 <sup>b-e</sup>	9.11 <sup>e</sup>		3.8 ± 0.03* <sup>d,e</sup>
Bi	70.97 <sup>f-g</sup>	8.78 <sup>g,i,f</sup>	4.72 ± 0.03* <sup>h</sup>	3.79 ± 0.07* <sup>h,g</sup>
S <sub>A</sub> <sup>j</sup>	109.53			3.83*
S <sub>B</sub> <sup>j</sup>	187.66	8.21 (A <sub>1</sub> )*	4.56 (A <sub>1</sub> )*	3.90*
		8.84 (E)*	4.8 (E)*	
S <sub>C</sub> <sup>j</sup>	370.49	7.61* <sup>k</sup>		3.75*
S <sub>D</sub> <sup>j</sup>	613.55	10.14*	5.13*	3.73*

<sup>a</sup>Ref. 12.

<sup>b</sup>Ref. 2.

<sup>c</sup>Ref. 3.

<sup>d</sup>Ref. 4.

<sup>e</sup>Ref. 5.

<sup>f</sup>Ref. 6.

<sup>g</sup>Ref. 7.

<sup>h</sup>Ref. 8.

<sup>i</sup>Ref. 9.

<sup>j</sup>Ref. 11, but see Ref. 10.

<sup>k</sup>Note that the direction of the shift due to central cell corrections is opposite to that expected.